Journal of the Serbian Chemical Society
JSCS@tmf.bg.ac.rs • www.shd.org.rs/JSCS
J. Serb. Chem. Soc. 90 (9) S356–S371 (2025) *Supplementary material*

SUPPLEMENTARY MATERIAL TO

Water-splitting electrocatalytic properties and computational characterization of a symmetrically substituted porphyrazine

MARINA ALEXANDRA TUDORAN and BOGDAN-OVIDIU TARANU*

National Institute of Research and Development for Electrochemistry and Condensed Matter, Dr. A. Paunescu Podeanu Street No. 144, 300569 Timisoara, Romania

J. Serb. Chem. Soc. 90 (9) (2025) 1089–1104

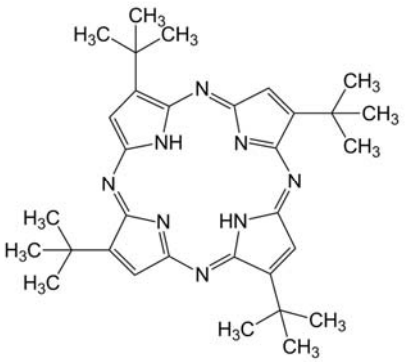

Scheme S-1. The chemical structure of 2,7,12,17-tetra-tert-butyl-5,10,15,20-tetraaza-21H,23H-porphine.

EQUATIONS

Equations employed in the electrochemical study

Equations (S-1) to (S-6) have been used during the study of the water-splitting electrocatalytic properties of 2,7,12,17-tetra-tert-butyl-5,10,15,20-tetraaza-21H,23H-porphine.[1-5]

Equation (S-1) is employed to represent the electrochemical potential value measured *vs.* the Ag/AgCl(sat. KCl) reference electrode in terms of the Reversible Hydrogen Electrode (RHE).

$$E_{RHE} = E_{Ag/AgCl(sat.\ KCl)} + 0.059\ \mathrm{pH} + E^{\circ}_{Ag/AgCl(sat.\ KCl)} \quad \text{(S-1)}$$

* Corresponding author. E-mail: b.taranu84@gmail.com

where E_{RHE} / V is the converted potential *vs.* RHE; $E_{Ag/AgCl(sat.\ KCl)}$ / V is the measured potential *vs.* the Ag/AgCl (sat. KCl) reference electrode and $E°_{Ag/AgCl(sat.\ KCl)}$ = 0.197 V.

Equation (S-2) is used to calculate the OER overpotential.

$$\eta_{OER} = E_{RHE} - 1.23 \quad \text{(S-2)}$$

where η_{OER} / V is the oxygen evolution overpotential.

Equation (S-3) is used to calculate the HER overpotential.

$$\eta_{HER} = |E_{RHE}| - 0 \quad \text{(S-3)}$$

where η_{HER} / V is the H_2 evolution overpotential.

Equation (S-4) is used to calculate the Tafel slope.

$$\eta = b \times \log(j) + a \quad \text{(S-4)}$$

where η / V is the overpotential; j / A cm^{-2} is the current density; b / V dec^{-1} is the Tafel slope and a is the exchange current density.

Equation (S-5) is used to calculate the capacitive current density.

$$j_{dl} = \frac{j_a + j_c}{2} \quad \text{(S-5)}$$

where j_{dl} / A cm^{-2} is the capacitive current density; j_a / A cm^{-2} is the absolute value of the anodic j at a given scan rate and at an E value from the range with only double-layer adsorption and desorption features and j_c / A cm^{-2} is the absolute value of the cathodic j at a given scan rate and at an E value from the range with only double-layer adsorption and desorption features.

Equation (S-6) is employed to estimate the electrochemically active surface area based on the electric double-layer capacitance. The latter is usually measured by recording cyclic voltammograms at various scan rate values followed by the determination of the slope of the curve from the graphical representation of the capacitive current density *vs.* the scan rate.

$$ECSA = \frac{C_{dl} \times S_{geom}}{C_s} \quad \text{(S-6)}$$

where $ECSA$ / cm^2 is the electrochemically active surface area; C_{dl} / F cm^{-2} is the electric double-layer capacitance; S_{geom} / cm^2 is the geometric surface of the electrode and C_s / F cm^{-2} is the specific capacitance of a smooth electrode surface.[6]

Equations employed in the theoretical study

The vertical ionization potential (*VIP*) and electron affinity (*VEA*) of a neutral system are calculated using the ΔSCF formalism, as the difference between the electronic energy of the cation and the electronic energy of the neutral molecule (Equation (S-7)), and the difference between the electronic energy of the neutral molecule and the electronic energy of the anion (Equation (S-8)), respectively.[7-9]

$$VIP = E_{cation} - E_{neutral} \quad \text{(S-7)}$$

$$VEA = E_{neutral} - E_{anion} \quad \text{(S-8)}$$

where $E_{neutral}$ is the electronic energy of the neutral molecule; E_{cation} is the electronic energy of the cation and E_{anion} is the electronic energy of the anion – the last two being evaluated at the geometry of the neutral molecule.

Polarizability (α):

$$\alpha = \frac{1}{3}\left(\alpha_{xx} + \alpha_{yy} + \alpha_{zz}\right) \quad \text{(S-9)}$$

Anisotropy of polarizability ($\Delta\alpha$):

$$\Delta\alpha = \frac{1}{\sqrt{2}}\left[\left(\alpha_{xx} - \alpha_{yy}\right)^2 + \left(\alpha_{yy} - \alpha_{zz}\right)^2 + (\alpha_{zz} - \alpha_{xx})^2 + 6\alpha_{xz}^2 + 6\alpha_{xy}^2 + 6\alpha_{yz}^2\right]^{1/2} \quad \text{(S-10)}$$

First hyperpolarizability (β):

$$\beta = \left[\left(\beta_{xxx} + \beta_{xyy} + \beta_{xzz}\right)^2 + \left(\beta_{yyy} + \beta_{yzz} + \beta_{yxx}\right)^2 + \left(\beta_{zzz} + \beta_{zxx} + \beta_{zyy}\right)^2\right]^{\frac{1}{2}} \quad \text{(S-11)}$$

To convert the values of polarizability, anisotropy of polarizability and hyperpolarizability measured in atomic units (a.u.) to electrostatic units (e.s.u.), the following formulas were used: for α, 1 a.u. = 0.1482×10^{-24} e.s.u., and for β, 1 a.u. = 8.6393×10^{-33}.

The equations were calculated using the x, y, z components from Gaussian 03W output, which are presented in Table S-V.

QUANTUM CHEMICAL CALCULATIONS

TABLE S-I. Calculated structural parameters of the optimized 2,7,12,17-tetra-tert-butyl-5,10,15,20-tetraaza-21H,23H-porphine

		Tetra-tert-butyl-tetraazaporphyrin			*Unfunctionalized porphyrazine*[a]
		B3LYP/ STO-3G	**B3PW91/ STO-3G**	**MPW1PW91/ STO-3G**	**B3LYP/ 6-31G(d)**
Bond length / Å	$C_{14} - C_{19}$	1.48709	1.48214	1.47895	1.453
	$C_{19} - C_{17}$	1.37053	1.36743	1.36392	1.378
	$C_{19} - C_{25}$	1.54594	1.53946	1.53573	-
	$C_{14} - N_{22}$	1.41549	1.40919	1.40511	1.371
	$C_{14} - N_{16}$	1.38882	1.38374	1.37953	1.323
	$N_{16} - C_{15}$	1.39013	1.38519	1.38099	1.338
	$N_{22} - H_{45}$	1.25823	1.25231	1.24972	-
	$C_{15} - C_{20}$	1.46894	1.46355	1.46111	1.475
	$N_{21} - C_{13}$	1.41526	1.40926	1.40493	1.361
	$C_{20} - H_{44}$	1.09331	1.09219	1.09037	-
Bond angle / °	$C_{17} - C_{19} - C_{14}$	105.51967	105.40852	105.42534	-
	$C_{19} - C_{14} - N_{22}$	110.73804	110.75401	110.76539	-
	$C_{14} - N_{16} - C_{15}$	113.74181	113.76580	113.82715	123.1
	$C_{14} - N_{22} - C_{12}$	105.78746	105.88973	105.89271	110.5
	$C_{15} - C_{20} - C_{18}$	107.80646	107.78086	107.71391	-
	$C_{15} - N_{21} - C_{13}$	105.71806	105.79135	105.80913	105.0

[a] Data from Mongale *et al.*[10]

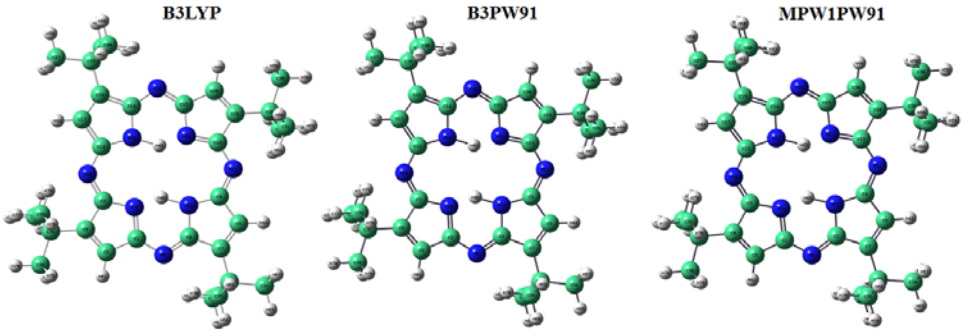

Fig. S-1. Optimized structure and atom labelling of 2,7,12,17-tetra-tert-butyl-5,10,15,20-tetraaza-21H,23H-porphine using STO-3G basis set.

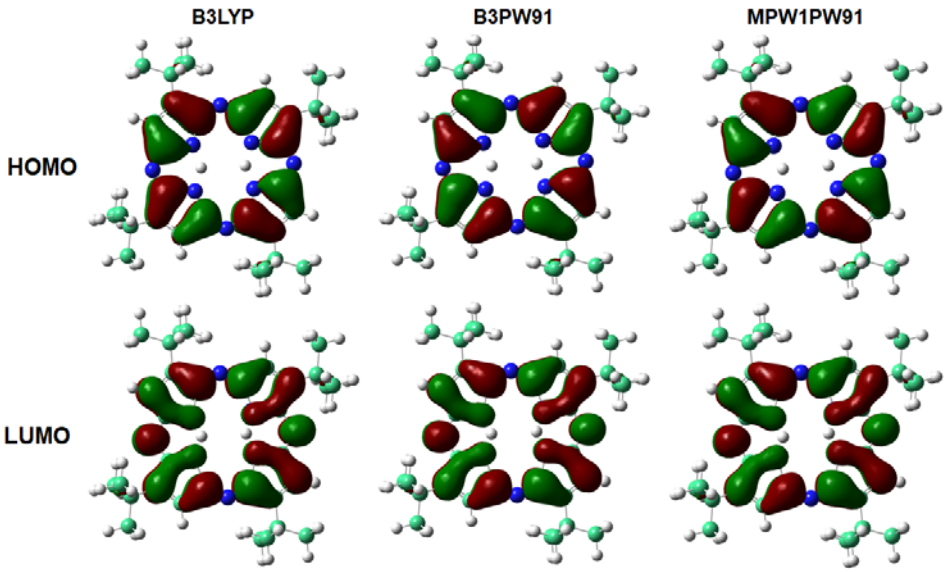

Fig. S-2. The atomic orbital composition of the HOMO and LUMO orbitals for 2,7,12,17-tetra-tert-butyl-5,10,15,20-tetraaza-21H,23H-porphine using 6-31G basis set.

TABLE S-II. Calculated energy values of HOMO (E_{HOMO}), LUMO (E_{LUMO}), energy gap (E_{gap}), vertical ionization potential and electron affinity of 2,7,12,17-tetra-tert-butyl-5,10,15,20-tetraaza-21H,23H-porphine.

Parameter	B3LYP/6-31G(d)	B3PW91/6-31G(d)	MPW1PW91/6-31G(d)
E_{HOMO} / eV	-5.497791	-5.699699	-5.619426
E_{LUMO} / eV	-3.194618	-3.161420	-3.287953
E_{gap} / eV	2.303173	2.538279	2.331473
VIP / eV	6.670086	6.781692	6.738326
VEA / eV	2.006947	2.10314	2.094558

TABLE S-III. Calculated thermodynamic parameters of 2,7,12,17-tetra-tert-butyl-5,10,15,20-tetraaza-21H,23H-porphine

Parameter		B3LYP/STO-3G	B3PW91/STO-3G	MPW1PW91/STO-3G
Zero-point vibrational energy / kcal mol^{-1}		466.29026	470.14528	474.06613
Total Electronic Energy with Zero-point correction		-1661.194191	-1660.787035	-1661.050020
Total Electronic Energy with Thermal energies		-1661.155169	-1660.748346	-1661.011627
Total Electronic Energy with Enthalpies		-1661.154225	-1660.747402	-1661.010683
Dipole moment / Debye		0.001500	0.000714	0.004386
Rotational constant / GHz	*X*	0.08238	0.08292	0.08339
	Y	0.07571	0.07614	0.07655
	Z	0.04092	0.04116	0.04139
Thermal energy / kcal mol^{-1}	**Total**	490.776	494.423	498.158
	Translational	0.889	0.889	0.889
	Rotational	0.889	0.889	0.889
	Vibrational	488.999	492.645	496.381
Constant volume heat capacity / cal mol-Kelvin^{-1}	**Total**	152.327	150.932	149.791
	Translational	2.981	2.981	2.981
	Rotational	2.981	2.981	2.981
	Vibrational	146.365	144.970	143.829
Entropy / cal mol-Kelvin^{-1}	**Total**	229.699	228.316	226.791
	Translational	44.736	44.736	44.736
	Rotational	38.374	38.356	38.339
	Vibrational	146.589	145.224	143.715

TABLE S-IV. Natural charge, population, and electronic configuration of 2,7,12,17-tetra-tert-butyl-5,10,15,20-tetraaza-21H,23H-porphine

	Atom	Natural charge	Natural population				Natural electronic configuration
			Core	*Valence*	*Rydberg*	*Total*	
B3LYP/6-31G(d)	**C14**	0.42413	1.99918	3.55160	0.02509	5.57587	[core]2S$^{(0.83)}$2p$^{(2.72)}$3p$^{(0.02)}$3d$^{(0.01)}$
	C19	-0.03832	1.99894	4.02020	0.01918	6.03832	[core]2S$^{(0.90)}$2p$^{(3.12)}$3p$^{(0.01)}$
	C17	-0.24989	1.99888	4.23900	0.01201	6.24989	[core]2S$^{(0.98)}$2p$^{(3.26)}$3p$^{(0.01)}$
	C25	-0.06437	1.99913	4.05314	0.01210	6.06437	[core]2S$^{(0.93)}$2p$^{(3.13)}$3p$^{(0.01)}$
	C15	0.41632	1.99925	3.55795	0.02647	5.58368	[core]2S$^{(0.84)}$2p$^{(2.72)}$3p$^{(0.02)}$3d$^{(0.01)}$
	C20	-0.26295	1.99884	4.25219	0.01191	6.26295	[core]2S$^{(0.97)}$2p$^{(3.28)}$3p$^{(0.01)}$
	C13	0.44709	1.99917	3.52796	0.02578	5.55291	[core]2S$^{(0.82)}$2p$^{(2.71)}$3p$^{(0.02)}$3d$^{(0.01)}$
	N22	-0.63946	1.99931	5.62598	0.01417	7.63946	[core]2S$^{(1.36)}$2p$^{(4.26)}$3p$^{(0.01)}$
	N16	-0.47341	1.99940	5.46035	0.01366	7.47341	[core]2S$^{(1.41)}$2p$^{(4.05)}$3p$^{(0.01)}$3d$^{(0.01)}$
	N21	-0.64084	1.99932	5.62720	0.01432	7.64084	[core]2S$^{(1.37)}$2p$^{(4.26)}$3p$^{(0.01)}$
	H44	0.25980	0.00000	0.73953	0.00067	0.74020	1S$^{(0.74)}$
	H41	0.25979	0.00000	0.73954	0.00067	0.74021	1S$^{(0.74)}$
B3PW91/6-31G(d)	**C14**	0.42194	1.99918	3.55368	0.02519	5.57806	[core]2S$^{(0.83)}$2p$^{(2.73)}$3p$^{(0.02)}$3d$^{(0.01)}$
	C19	-0.03970	1.99895	4.02155	0.01920	6.03970	[core]2S$^{(0.89)}$2p$^{(3.13)}$3p$^{(0.01)}$
	C17	-0.25715	1.99888	4.24619	0.01208	6.25715	[core]2S$^{(0.98)}$2p$^{(3.27)}$3p$^{(0.01)}$
	C25	-0.07279	1.99913	4.06194	0.01172	6.07279	[core]2S$^{(0.92)}$2p$^{(3.14)}$3p$^{(0.01)}$
	C15	0.41300	1.99925	3.56120	0.02655	5.58700	[core]2S$^{(0.97)}$2p$^{(3.28)}$3p$^{(0.01)}$
	C20	-0.27005	1.99885	4.25913	0.01208	6.27005	[core]2S$^{(0.82)}$2p$^{(2.71)}$3p$^{(0.02)}$3d$^{(0.01)}$
	C13	0.44546	1.99917	3.52938	0.02599	5.55454	[core]2S$^{(1.36)}$2p$^{(4.27)}$3p$^{(0.01)}$
	N22	-0.63824	1.99930	5.62433	0.01461	7.63824	[core]2S$^{(1.41)}$2p$^{(4.05)}$3p$^{(0.01)}$3d$^{(0.01)}$
	N16	-0.46988	1.99939	5.45645	0.01403	7.46988	[core]2S$^{(1.41)}$2p$^{(4.05)}$3p$^{(0.01)}$3d$^{(0.01)}$
	N21	-0.63983	1.99932	5.62573	0.01479	7.63983	[core]2S$^{(1.36)}$2p$^{(4.26)}$3p$^{(0.01)}$
	H44	0.26763	0.00000	0.73172	0.00065	0.73237	1S$^{(0.73)}$
	H41	0.26763	0.00000	0.73172	0.00065	0.73237	1S$^{(0.73)}$
MPW1PW91/6-31G(d)	**C14**	0.42661	1.99918	3.54854	0.02566	5.57339	[core]2S$^{(0.82)}$2p$^{(2.72)}$3p$^{(0.02)}$3d$^{(0.01)}$
	C19	-0.03982	1.99895	4.02124	0.01963	6.03982	[core]2S$^{(0.89)}$2p$^{(3.13)}$3p$^{(0.01)}$
	C17	-0.25830	1.99888	4.24700	0.01242	6.25830	[core]2S$^{(0.98)}$2p$^{(3.27)}$3p$^{(0.01)}$
	C25	-0.07408	1.99913	4.06313	0.01183	6.07408	[core]2S$^{(0.92)}$2p$^{(3.14)}$3p$^{(0.01)}$
	C15	0.41772	1.99925	3.55592	0.02710	5.58228	[core]2S$^{(0.83)}$2p$^{(2.73)}$3p$^{(0.02)}$3d$^{(0.01)}$
	C20	-0.27099	1.99884	4.25972	0.01243	6.27099	[core]2S$^{(0.97)}$2p$^{(3.29)}$3p$^{(0.01)}$
	C13	0.45025	1.99917	3.52411	0.02648	5.54975	[core]2S$^{(0.81)}$2p$^{(2.71)}$3p$^{(0.02)}$3d$^{(0.01)}$
	N22	-0.64418	1.99930	5.62998	0.01490	7.64418	[core]2S$^{(1.35)}$2p$^{(4.28)}$3p$^{(0.01)}$
	N16	-0.47430	1.99939	5.46058	0.01434	7.47430	[core]2S$^{(1.40)}$2p$^{(4.06)}$3p$^{(0.01)}$3d$^{(0.01)}$
	N21	-0.64574	1.99931	5.63136	0.01507	7.64574	[core]2S$^{(1.36)}$2p$^{(4.27)}$3p$^{(0.01)}$
	H44	0.26824	0.00000	0.73111	0.00065	0.73176	1S$^{(0.73)}$
	H41	0.26824	0.00000	0.73112	0.00065	0.73176	1S$^{(0.73)}$

TABLE S-V. Polarizability, anisotropy of polarizability, first hyperpolarizability and their components of 2,7,12,17-tetra-tert-butyl-5,10,15,20-tetraaza-21H,23H-porphine

DFT	**B3LYP/6-31G(d)**	**B3PW91/6-31G(d)**	**MPW1PW91/6-31G(d)**
α_{xx}	698.6429625	693.2942536	686.7598955
α_{xy}	-5.9861099	6.0337992	-5.8576367
α_{yy}	673.8693311	668.4113409	662.2107292
α_{xz}	0.0030171	-0.0019439	0.0032899
α_{yz}	0.0047666	0.0079143	0.0004745
α_{zz}	232.3156124	232.2472824	230.59394
α / e.s.u.	$7.927849856 \times 10^{-23}$	$7.874127212 \times 10^{-23}$	$7.80304895 \times 10^{-23}$
$\Delta\alpha$/ e.s.u.	$6.736660958 \times 10^{-23}$	$6.657801463 \times 10^{-23}$	$6.587727255 \times 10^{-23}$
β_{xxx}	-20.3999455	-22.8725558	-5.0131258
β_{xxy}	10.9304831	-4.595366	-2.0657743
β_{xyy}	0.2712327	2.8787402	-2.0809949
β_{yyy}	-25.2245749	-50.1636542	-26.9530695
β_{xxz}	10.4942587	2.7133526	3.1471885
β_{yyz}	11.155742	21.1487207	12.7231708
β_{xzz}	-4.3206832	0.7108711	-2.8860579
β_{yzz}	-4.4919258	-8.0685999	-4.9231165
β_{zzz}	-0.4285422	0.1992636	-0.3401646
β / e.s.u.	$3.233727869 \times 10^{-31}$	$6.046331071 \times 10^{-31}$	$3.337999671 \times 10^{-31}$

ELECTROCHEMICAL STUDY

Voltammetry results

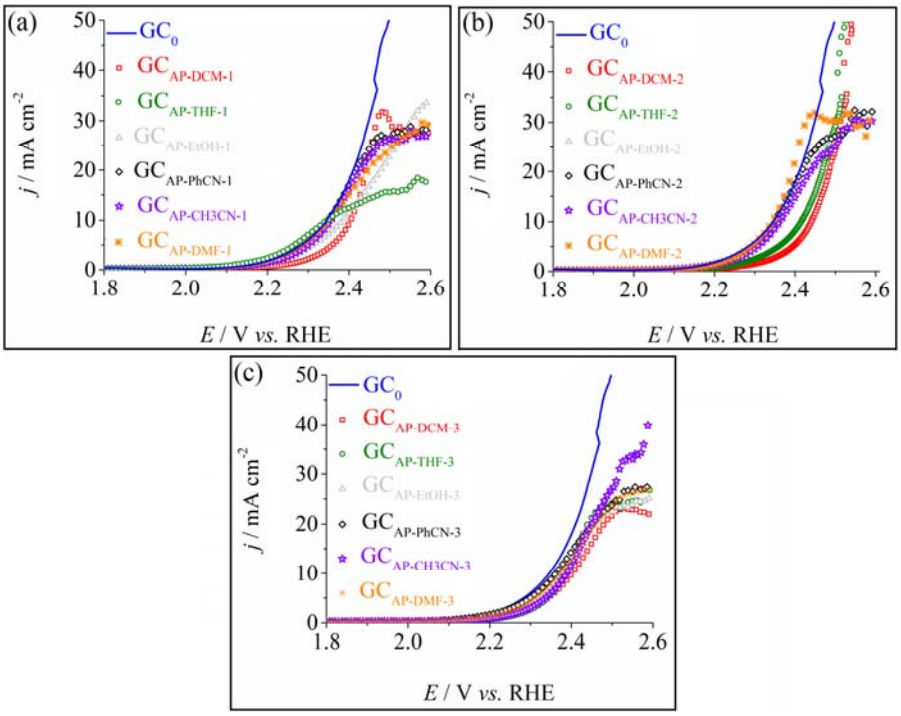

Fig. S-3. Anodic LSVs obtained on GC_0 and on (a) $GC_{AP-DCM-1}$, $GC_{AP-THF-1}$, $GC_{AP-EtOH-1}$, $GC_{AP-PhCN-1}$, $GC_{AP-CH3CN-1}$ and $GC_{AP-DMF-1}$; (b) $GC_{AP-DCM-2}$, $GC_{AP-THF-2}$, $GC_{AP-EtOH-2}$, $GC_{AP-PhCN-2}$, $GC_{AP-CH3CN-2}$ and $GC_{AP-DMF-2}$ and (c) $GC_{AP-DCM-3}$, $GC_{AP-THF-3}$, $GC_{AP-EtOH-3}$, $GC_{AP-PhCN-3}$, $GC_{AP-CH3CN-3}$ and $GC_{AP-DMF-3}$. Electrolyte solution: 0.1 mol L^{-1} H_2SO_4. v = 5 mV s^{-1}.

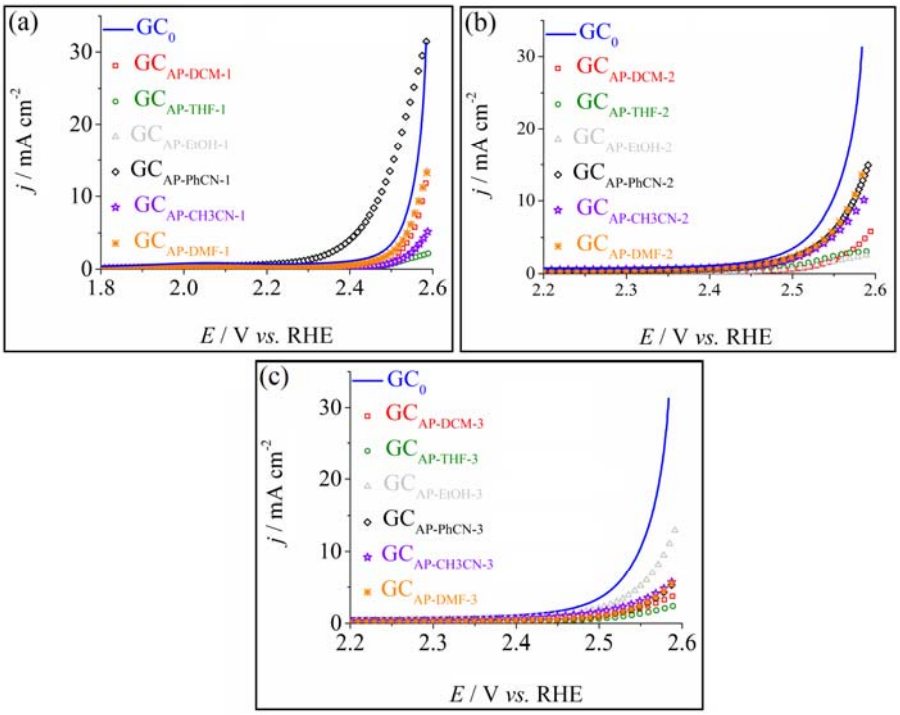

Fig. S-4. Anodic LSVs obtained on GC_0 and on (a) $GC_{AP\text{-}DCM\text{-}1}$, $GC_{AP\text{-}THF\text{-}1}$, $GC_{AP\text{-}EtOH\text{-}1}$, $GC_{AP\text{-}PhCN\text{-}1}$, $GC_{AP\text{-}CH3CN\text{-}1}$ and $GC_{AP\text{-}DMF\text{-}1}$; (b) $GC_{AP\text{-}DCM\text{-}2}$, $GC_{AP\text{-}THF\text{-}2}$, $GC_{AP\text{-}EtOH\text{-}2}$, $GC_{AP\text{-}PhCN\text{-}2}$, $GC_{AP\text{-}CH3CN\text{-}2}$ and $GC_{AP\text{-}DMF\text{-}2}$ and (c) $GC_{AP\text{-}DCM\text{-}3}$, $GC_{AP\text{-}THF\text{-}3}$, $GC_{AP\text{-}EtOH\text{-}3}$, $GC_{AP\text{-}PhCN\text{-}3}$, $GC_{AP\text{-}CH3CN\text{-}3}$ and $GC_{AP\text{-}DMF\text{-}3}$. Electrolyte solution: 0.1 mol L^{-1} KCl. v = 5 mV s^{-1}.

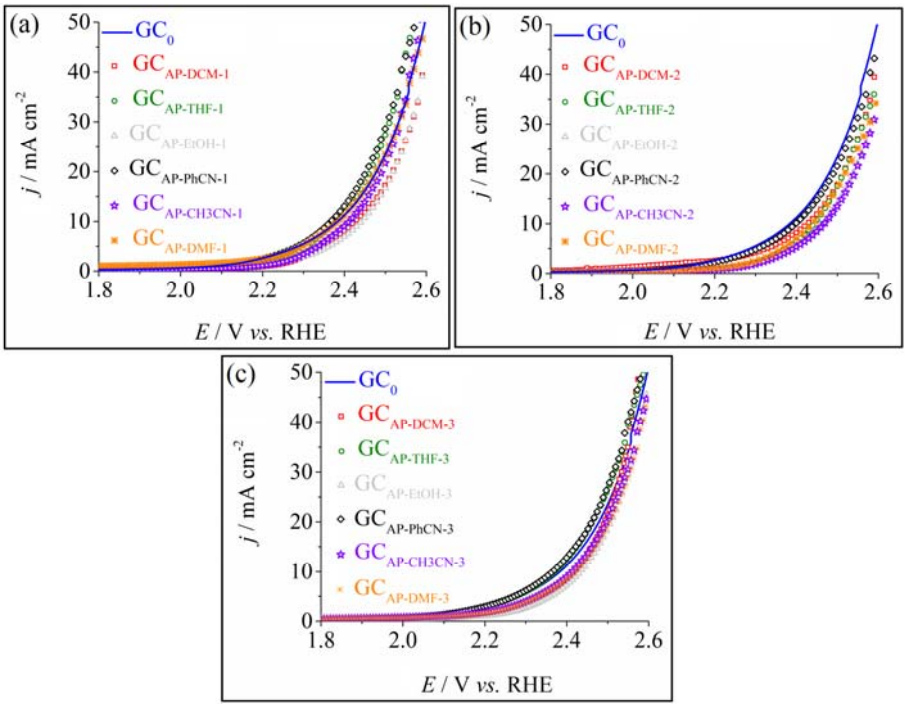

Fig. S-5. Anodic LSVs obtained on GC_0 and on (a) $GC_{AP-DCM-1}$, $GC_{AP-THF-1}$, $GC_{AP-EtOH-1}$, $GC_{AP-PhCN-1}$, $GC_{AP-CH3CN-1}$ and $GC_{AP-DMF-1}$; (b) $GC_{AP-DCM-2}$, $GC_{AP-THF-2}$, $GC_{AP-EtOH-2}$, $GC_{AP-PhCN-2}$, $GC_{AP-CH3CN-2}$ and $GC_{AP-DMF-2}$ and (c) $GC_{AP-DCM-3}$, $GC_{AP-THF-3}$, $GC_{AP-EtOH-3}$, $GC_{AP-PhCN-3}$, $GC_{AP-CH3CN-3}$ and $GC_{AP-DMF-3}$. Electrolyte solution: 1 mol L^{-1} KOH. v = 5 mV s^{-1}.

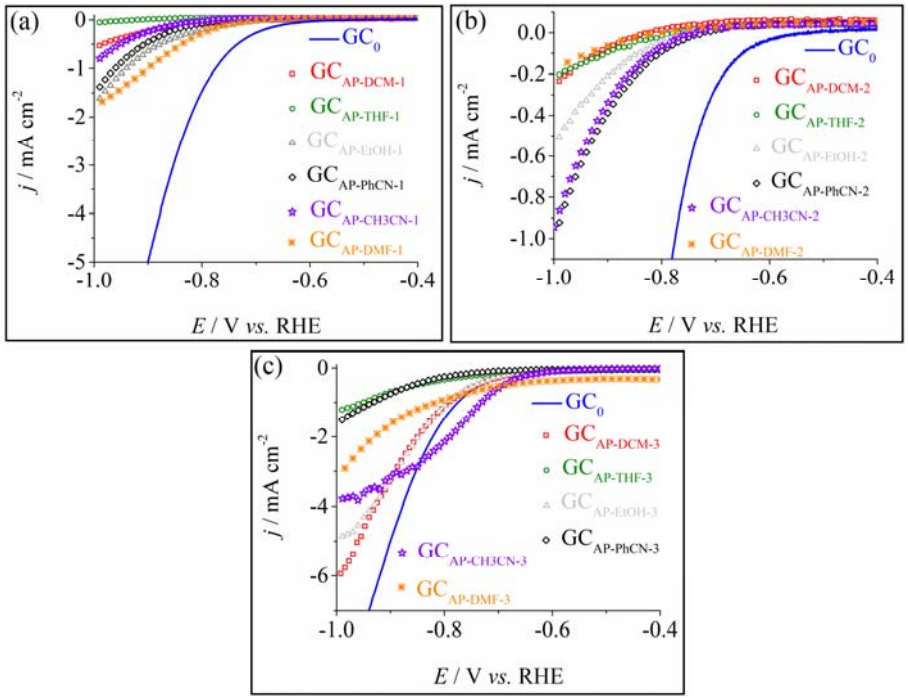

Fig. S-6. Cathodic LSVs obtained on GC_0 and on (a) $GC_{AP\text{-}DCM\text{-}1}$, $GC_{AP\text{-}THF\text{-}1}$, $GC_{AP\text{-}EtOH\text{-}1}$, $GC_{AP\text{-}PhCN\text{-}1}$, $GC_{AP\text{-}CH3CN\text{-}1}$ and $GC_{AP\text{-}DMF\text{-}1}$; (b) $GC_{AP\text{-}DCM\text{-}2}$, $GC_{AP\text{-}THF\text{-}2}$, $GC_{AP\text{-}EtOH\text{-}2}$, $GC_{AP\text{-}PhCN\text{-}2}$, $GC_{AP\text{-}CH3CN\text{-}2}$ and $GC_{AP\text{-}DMF\text{-}2}$ and (c) $GC_{AP\text{-}DCM\text{-}3}$, $GC_{AP\text{-}THF\text{-}3}$, $GC_{AP\text{-}EtOH\text{-}3}$, $GC_{AP\text{-}PhCN\text{-}3}$, $GC_{AP\text{-}CH3CN\text{-}3}$ and $GC_{AP\text{-}DMF\text{-}3}$. Electrolyte solution: 0.1 mol L^{-1} H_2SO_4. v = 5 mV s^{-1}.

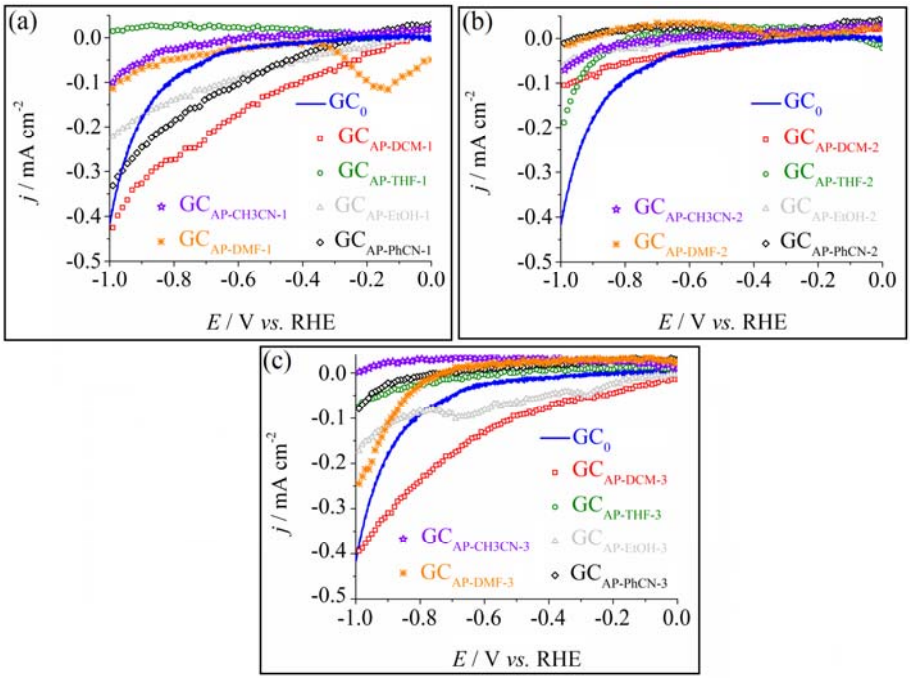

Fig. S-7. Cathodic LSVs obtained on GC_0 and on (a) $GC_{AP\text{-}DCM\text{-}1}$, $GC_{AP\text{-}THF\text{-}1}$, $GC_{AP\text{-}EtOH\text{-}1}$, $GC_{AP\text{-}PhCN\text{-}1}$, $GC_{AP\text{-}CH3CN\text{-}1}$ and $GC_{AP\text{-}DMF\text{-}1}$; (b) $GC_{AP\text{-}DCM\text{-}2}$, $GC_{AP\text{-}THF\text{-}2}$, $GC_{AP\text{-}EtOH\text{-}2}$, $GC_{AP\text{-}PhCN\text{-}2}$, $GC_{AP\text{-}CH3CN\text{-}2}$ and $GC_{AP\text{-}DMF\text{-}2}$ and (c) $GC_{AP\text{-}DCM\text{-}3}$, $GC_{AP\text{-}THF\text{-}3}$, $GC_{AP\text{-}EtOH\text{-}3}$, $GC_{AP\text{-}PhCN\text{-}3}$, $GC_{AP\text{-}CH3CN\text{-}3}$ and $GC_{AP\text{-}DMF\text{-}3}$. Electrolyte solution: 0.1 mol L^{-1} KCl. v = 5 mV s^{-1}.

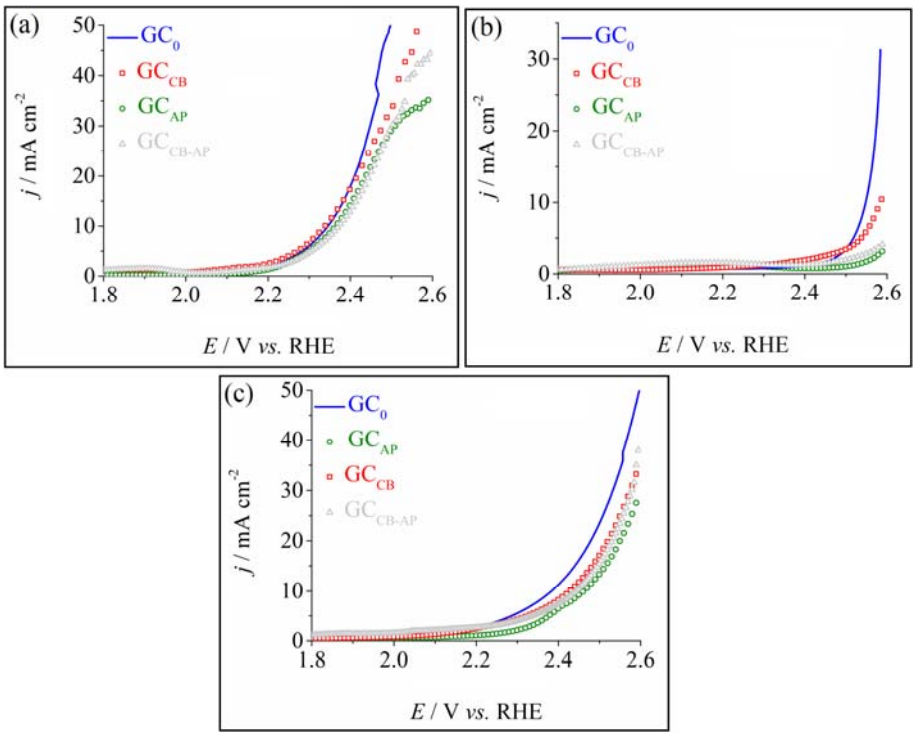

Fig. S-8. Anodic LSVs obtained on GC_0, GC_{CB}, GC_{AP} and GC_{CB-AP} in the following electrolyte solutions: (a) 0.1 mol L^{-1} H_2SO_4, (b) 0.1 mol L^{-1} KCl and (c) 1 mol L^{-1} KOH. v = 5 mV s^{-1}.

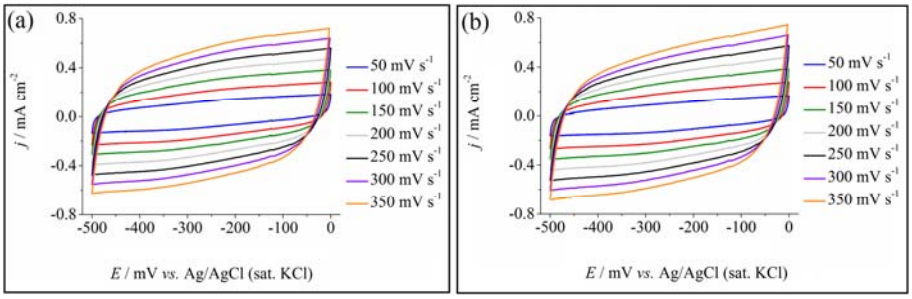

Fig. S-9. (a and b) CVs obtained on two GC_{CB-AP} electrodes in the E range from -500 to 0 mV, at increasing v values (50, 100, 150, 200, 250, 300 and 350 mV s^{-1}). Electrolyte solution: 0.1 mol L^{-1} KCl.

Raman spectra

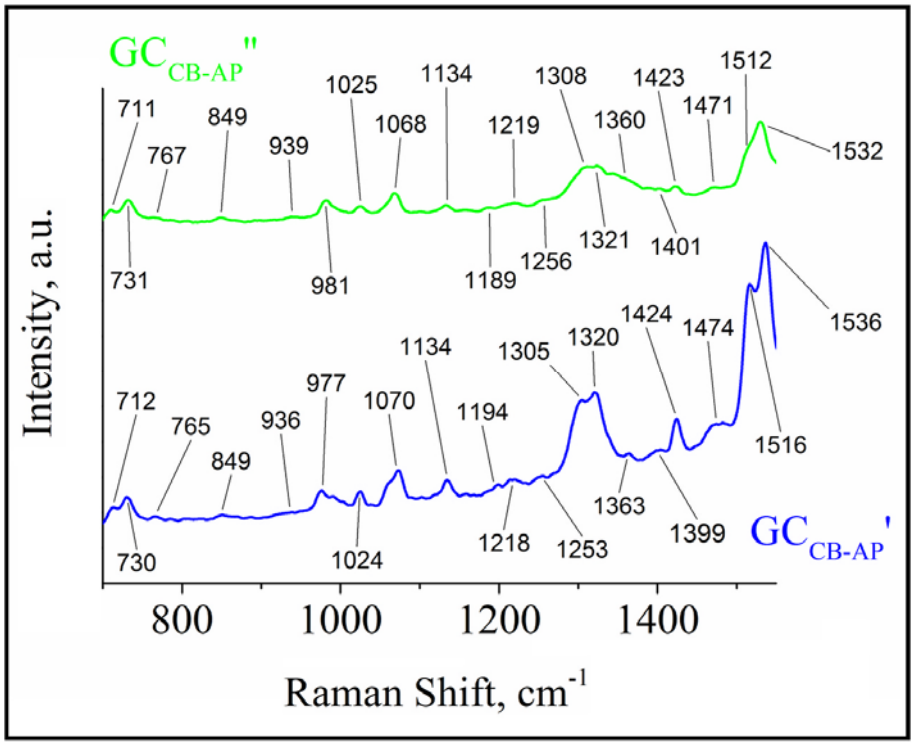

Fig. S-10. Raman spectra recorded on GC_{CB-AP} before a chronoamperometric stability test performed in 1 mol L^{-1} KOH solution (GC_{CB-AP}') and after the test (GC_{CB-AP}").

Statistical analysis

Before conducting the correlation analysis, a preliminary investigation was undertaken to ascertain the normality of the studied variables. This was achieved by employing a One-Sample Kolmogorov-Smirnov test. In the case of OER, the data for overpotential ($D(47) = 1.096$, $p > 0.05$) and polarity ($D(47) = 1.170$, $p > 0.05$) exhibited a normal distribution, while the data for pH ($D(47) = 1.856$, $p < 0.05$) and the number of layers ($D(47) = 1.778$, $p < 0.05$) were found to be non-normally distributed. Based on these results, Pearson statistics were computed to assess the relationship between overpotential and polarity, while Spearman's Rho statistic was computed to evaluate the relationship between the overpotential, the pH, and the number of layers. The results indicate no statistically significant correlation between overpotential, polarity, and number of layers. However, Spearman's correlation coefficient was found to be statistically significant for overpotential and pH (r_S (45) = 0.447, p < 0.01), thereby revealing a positive association between them. In the case of HER, the results of the One-Sample

Kolmogorov-Smirnov test show that the data for overpotential ($D(23) = 0.668$, $p > 0.05$), polarity ($D(23) = 0.847$, $p > 0.05$), and number of layers ($D(23) = 1.359$, $p = 0.05$) follow a normal distribution, whilst the pH data ($D(23) = 1.665$, $p < 0.05$) were found to be non-normally distributed. Based on these results, Pearson's statistics were computed to assess the relationships between overpotential, polarity, and number of layers, while Spearman's rho statistics were computed for the relationship between overpotential and pH. The obtained results revealed no statistically significant correlation between the overpotential and the other variables examined in the study.

REFERENCES

1. B.-R. Wulan, S.-S. Yi, S.-J. Li, Y.-X. Duan, J.-M. Yan, X.-B. Zhang, Q. Jiang, *Mater. Chem. Front.* **2** (2018) 1799 (https://doi.org/10.1039/C8QM00239H)
2. Raveendran, M. Chandran, R. Dhanusuraman, *RSC Adv.* **13** (2023) 3843 (https://doi.org/10.1039/D2RA07642J)
3. O. van der Heijden, S. Park, R. E. Vos, J. J. J. Eggebeen, M. T. M. Koper, *ACS Energy Lett.* **9** (2024) 1871 (https://doi.org/10.1021/acsenergylett.4c00266)
4. O. Taranu, S. D. Novaconi, M. Ivanovici, J. N. Goncalves, F. S. Rus, *Appl. Sci.-Basel* **12** (2022) 1 (https://doi.org/10.3390/app12136821)
5. Karmakar, S. Kundu, *Mater. Today Energy* **33** (2023) 1 (https://doi.org/10.1016/j.mtener.2023.101259)
6. M. L. F. Ciriaco, M. I. Silva-Pereira, M. R. Nunes, F. M. Costa, *Port. Electrochim. Acta* **17** (1999) 149 (https://doi.org/10.4152/pea.199902149)
7. V. Lemierre, A. Chrostowska, A. Dargelos, H. Chermette, *J. Phys. Chem. A* **109** (2005) 8348 (https://doi.org/10.1021/jp050254c)
8. P. Vibert, D. J. Tozer, *J. Chem. Theory Comput.* **15** (2018) 241 (https://doi.org/10.1021/acs.jctc.8b00938)
9. L. A. Curtiss, P. C. Redfern, K. Raghavachari, J. A. Pople, *J. Chem. Phys.* **109** (1998) 42 (https://doi.org/10.1063/1.476538)
10. M. K. Mongale, D. A. Isabirye, M. M. Kabanda, T. O. Aiyelabola, E. E. Ebenso, *Asian J. Chem.* **29** (2017) 496 (https://doi.org/10.14233/ajchem.2017.20205).